High-Resolution Mapping of the Novel Early Leaf Senescence Gene *Els2* in Common Wheat

Na Wang †, Yanzhou Xie *,†, Yingzhuang Li, Shengnan Wu, Shuxian Li, Yu Guo and Chengshe Wang *

State Key Laboratory of Crop Stress Biology for Arid Areas, College of Agronomy, Northwest A&F University, Yangling 712100, China; wangnawheat@163.com (N.W.); lyz13077031@163.com (Y.L.); wushengnan666@163.com (S.W.); lishuxian0706@163.com (S.L.); gy15598128707@163.com (Y.G.)

* Correspondence: yzxie@nwafu.edu.cn (Y.X.); wangcs2008@126.com (C.W.)

† These authors contributed equally to this work.

Abstract: Early leaf senescence negatively impacts the grain yield in wheat (*Triticum aestivum* L.). Induced mutants provide an important resource for mapping and cloning of genes for early leaf senescence. In our previous study, *Els2*, a single incomplete dominance gene, that caused early leaf senescence phenotype in the wheat mutant LF2099, had been mapped on the long arm of chromosome 2B. The objective of this study was to develop molecular markers tightly linked to the *Els2* gene and construct a high-resolution map surrounding the *Els2* gene. Three tightly linked single-nucleotide polymorphism (SNP) markers were obtained from the Illumina Wheat 90K iSelect SNP genotyping array and converted to Kompetitive allele-specific polymerase chain reaction (KASP) markers. To saturate the *Els2* region, the Axiom®Wheat 660K SNP array was used to screen bulked extreme phenotype DNA pools, and 9 KASP markers were developed. For fine mapping of the *Els2* gene, these KASP markers and previously identified polymorphic markers were analyzed in a large F_2 population of the LF2099 × Chinese Spring cross. The *Els2* gene was located in a 0.24-cM genetic region flanked by the KASP markers AX-111643885 and AX-111128667, which corresponded to a physical interval of 1.61 Mb in the Chinese Spring chromosome 2BL containing 27 predicted genes with high confidence. The study laid a foundation for a map-based clone of the *Els2* gene controlling the mutation phenotype and revealing the molecular regulatory mechanism of wheat leaf senescence.

Keywords: wheat (*Triticum aestivum* L.); early leaf senescence; mutant; single-nucleotide polymorphisms (SNPs); KASP markers; fine mapping

1. Introduction

Wheat is one of the most widely grown crops in the world, providing more than 20% of the calories and protein consumed by the human population [1]. Maintaining a high and stable yield of wheat cultivars is a huge challenge for both wheat breeders and researchers. Leaves are the main photosynthetic organ of wheat plants. A previous study showed that the photosynthetically active flag leaf can contribute 30%–50% of the assimilates for grain filling and yield [2]. The early senescence of functional leaves significantly reduces photosynthetic time and efficiency, seriously affecting grain yield and quality in wheat [3]. Therefore, discovering the genes responsible for early leaf senescence is important not only for the elucidation of the early leaf senescence mechanism, but also in terms of its applications in the development of wheat germplasms and cultivars.

Plant leaf senescence involves a complex and highly regulated process with the coordinated actions of multiple pathways [4,5]. In recent years, researchers have elucidated the molecular mechanisms of leaf senescence in model plants, and isolated and characterized several senescence-associated genes that

are involved in chlorophyll (Chl) degradation [6–9], reactive oxygen species (ROS) scavenging [10–12], carbon and nitrogen imbalances [13–15], and hormone responses [16–20]. However, limited information is available about leaf senescence regulation in wheat. Several studies focused on the transcriptome of wheat leaf senescence [21–24]. These studies have provided global and potential gene dynamic expression changes and signalling pathways for leaf senescence regulation in wheat, but few genes involved in the regulation of wheat leaf senescence have been identified. Several early leaf senescence mutant genes in wheat were mapped using molecular markers [3,25,26]; however, our understanding of the molecular mechanism of the leaf senescence trait in wheat is limited because none of these genes have been fine mapped and cloned.

The induced mutants have also become important for forward genetic analysis, where genes underlying mutant traits can be mapped using molecular markers [25]. Various classes of molecular markers, particularly simple sequence repeat (SSR) markers, have been widely used to identify mutant genes in wheat [27–31]. However, it is difficult to develop a high-resolution genetic linkage map based only on SSR markers because of their limited number and scattered distribution on wheat chromosomes. Single-nucleotide polymorphisms (SNPs) are the most abundant type of molecular marker in plant, and a large number of SNPs have been discovered in wheat with the improvement of sequencing techniques [32–36]. At present, several kinds of wheat SNP arrays have been reported, such as the Illumina Wheat 9K iSelect SNP array [37], the Illumina Wheat 90K iSelect SNP genotyping array [38], the Axiom®HD Wheat genotyping (820K) array [39], the Wheat Breeders' 35K Axiom array [40], 660K [34] and the Wheat 55K SNP array [41]. The 660K SNP array [42] has been effectively applied to develop Kompetitive allele-specific polymerase chain reaction (KASP) markers for saturation mapping of the target genes. Examples include the molecular mapping of the dwarfing genes *Rht12* [43] and *Rht24* [44], stripe rust resistances *Yr26* [45], *YrH62* [46] and *Qyrnap.nwafu-2BS* [47], and the chlorina mutant gene *cn-A1* [48].

We previously reported the first case of the early leaf senescence mutant in wheat, which was controlled by the single incomplete dominant gene *Els2* [49]. The *Els2* gene was preliminarily mapped on chromosome arm 2BL in a 0.95 cM genetic interval between intron polymorphism (IP) markers 2BIP09 and 2BIP14 [49]. The objectives of this study were (1) to develop molecular markers closely linked to *Els2* using the wheat 660K SNP array, and (2) to construct a high-resolution linkage map.

2. Results

2.1. Development of Kompetitive Allele-Specific Polymerase Chain Reaction (KASP) Markers Based on the 90K Single-Nucleotide Polymorphisms (SNP) Array

Previously, the early leaf senescence *Els2* gene was mapped to chromosome 2BL using the Illumina wheat 90K SNP array [49]. Given that the SNP array has limitations in large scale population analysis, 15 chromosome-specific SNPs generated from 90K SNP were converted into 11 KASP primer pairs. They were subjected to a polymorphism analysis on the parental cultivars and 20 F_2 plants (including six homozygous wide type, eight heterozygous, and six homozygous mutant plants). Three polymorphic KASP markers (BS00030364_51, BS00084417_51 and RFL_Contig4423_529) were identified (Figure 1A). By genotyping the previous mapping population consisting of 142 $F_{2:3}$ lines from the LF2099 × Chinese Spring cross [49], all three KASP markers linked to the *Els2* gene (Figure 1C, Table 1). The *Els2* gene was then genetically restricted to a region of 1.1 cM, 0.54 cM from the KASP marker BS00084417_51 and 0.66 cM from the KASP marker RFL_Contig4423_529 (Figure 2A). However, the *Els2* genetic region were not narrowed down by using KASP markers from the 90K SNP array.
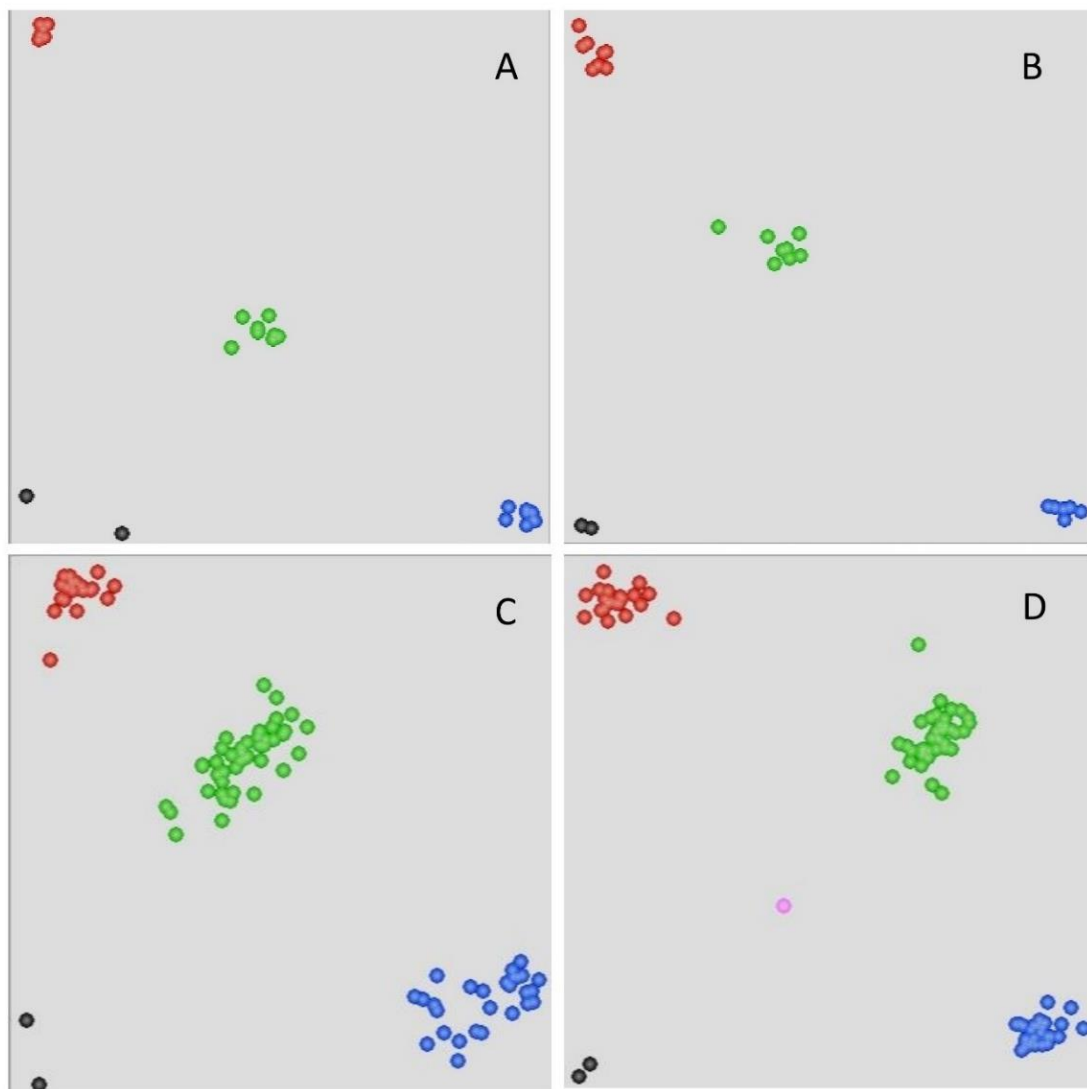
Figure 1. Genotypic plots from selected Kompetitive allele-specific polymerase chain reaction (KASP) assays. The results of the parents and small population using markers (**A**) BS00084417_51 and (**B**) AX-111128667. Results of the F_2 population using markers (**C**) RFL_Contig4423_529 and (**D**) AX-95682571. The central cluster (green) comprises heterozygous individuals, whereas the clusters near the axes are homozygous for either LF2099 (red) or Chinese Spring (blue). The black dots represent the nontemplate control, and the pink dots represent missing or failed data.

Table 1. Primer sequences of Kompetitive allele-specific polymerase (KASP) markers developed from the 90K and 660K arrays.

| Sources	Marker Name (SNP ID)	Primer Sequences (5′–3′)
90K	BS00030364_51	Forward A_FAM: GAAGGTGACCAAGTTCATGCTACAGCCAAAGACCCATCTTAA Forward B_HEX: GAAGGTCGGAGTCAACGGATTACAGCCAAAGACCCATCTTAG Common reverse: GTGCGAACAGTTGACAGTGA
90K	BS00084417_51	Forward A_FAM: GAAGGTGACCAAGTTCATGCTGCTGGAACTCGCCTCTTCTA Forward B_HEX: GAAGGTCGGAGTCAACGGATTGCTGGAACTCGCCTCTTCTC Common reverse: ATTTCAGCCCATCATCCTCC
90K	RFL_Contig4423_529	Forward A_FAM: GAAGGTGACCAAGTTCATGCTCATACTCACAGTAACAGATTGCAT Forward B_HEX: GAAGGTCGGAGTCAACGGATTCATACTCACAGTAACAGATTGCAC Common reverse: GCTTCTGCCACAAGCTCT
660K	AX-94995576	Forward A_FAM: GAAGGTGACCAAGTTCATGCTCGTGCATCTAAACCCACGTATA Forward B_HEX: GAAGGTCGGAGTCAACGGATTCGTGCATCTAAACCCACGTATC Common reverse: AGAGTCTCTATACCGTGATCCG
660K	AX-95682571	Forward A_FAM: GAAGGTGACCAAGTTCATGCTATGTGTGGTTCCATTCACCG Forward B_HEX: GAAGGTCGGAGTCAACGGATTATGTGTGGTTCCATTCACCA Common reverse: CAAGTCTGAGTGGAAGAAGGAC
660K	AX-111595417	Forward A_FAM: GAAGGTGACCAAGTTCATGCTTTCAGAAGAAATAGATGTATGTGCC Forward B_HEX: GAAGGTCGGAGTCAACGGATTTTCAGAAGAAATAGATGTATGTGCA Common reverse: CCATCCCATAAACCCAGGG
660K	AX-94859941	Forward A_FAM: GAAGGTGACCAAGTTCATGCTCCTCAGCTTTCTTTAGGGCT Forward B_HEX: GAAGGTCGGAGTCAACGGATTCCTCAGCTTTCTTTAGGGCC Common reverse: AATTCCGGTTCACTGGTCCA
660K	AX-111600462	Forward A_FAM: GAAGGTGACCAAGTTCATGCTCCAAAAATAAATTCCGCTAGTCCT Forward B_HEX: GAAGGTCGGAGTCAACGGATTCCAAAAATAAATTCCGCTAGTCCC Common reverse: CCAAAAACCCAATTGCAAGGTTAA
660K	AX-111497410	Forward A_FAM: GAAGGTGACCAAGTTCATGCTGAATGCAAAGGTTGGCCCT Forward B_HEX: GAAGGTCGGAGTCAACGGATTGAATGCAAAGGTTGGCCCG Common reverse: CTCGTGCGTACCTGCTCATT
660K	AX-109407129	Forward A_FAM: GAAGGTGACCAAGTTCATGCTTCTTGCCACCGTTTCAATAGAT Forward B_HEX: GAAGGTCGGAGTCAACGGATTTCTTGCCACCGTTTCAATAGAC Common reverse: CTTTTCTTGGTCTATGTAGTTGGG
660K	AX-111128667	Forward A_FAM: GAAGGTGACCAAGTTCATGCTGCGGGCAAAGCTTTGGATG Forward B_HEX: GAAGGTCGGAGTCAACGGATTGCGGGCAAAGCTTTGGATA Common reverse: GAGGTAGCGACGATGTCCC
660K	AX-111643885	Forward A_FAM: GAAGGTGACCAAGTTCATGCTGATGCAAATCCAAACCCATTCT Forward B_HEX: GAAGGTCGGAGTCAACGGATTGATGCAAATCCAAACCCATTCG Common reverse: GCAGGAGGAGAGCTTGGGA
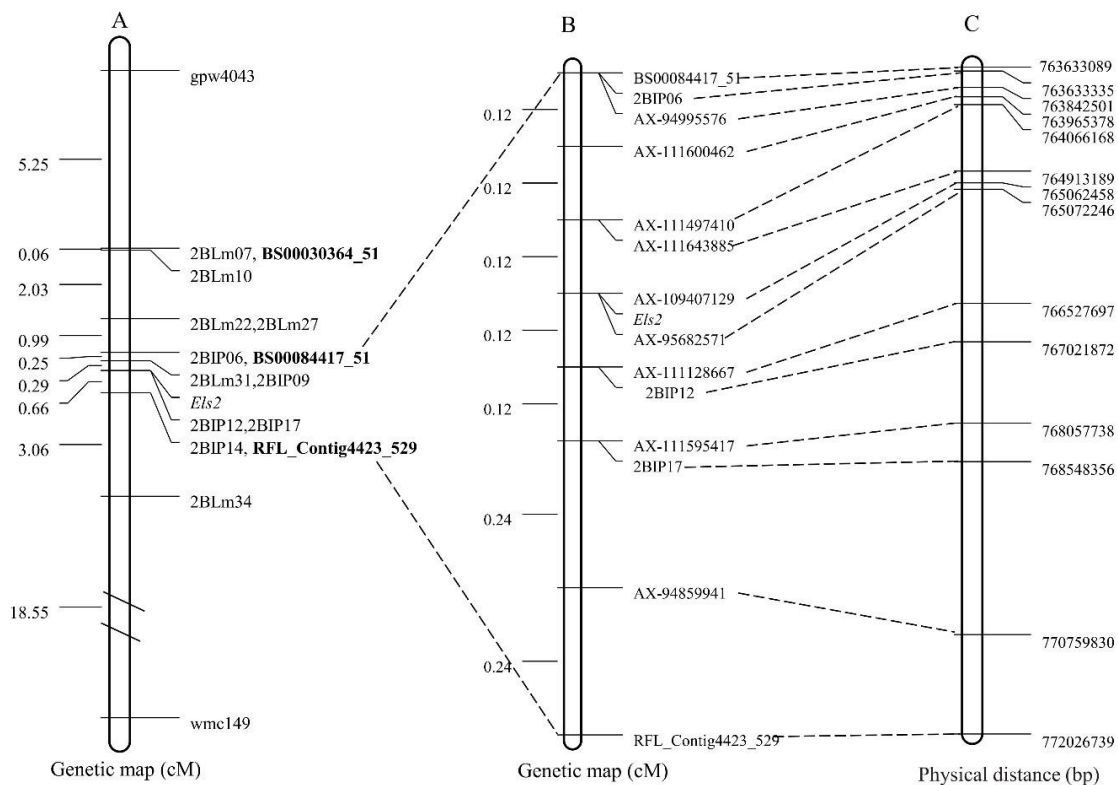
Figure 2. The genetic linkage map and physical map of Chinese Spring genomic sequence fanking the *Els2* gene. (**A**) The preliminary genetic linkage map of the *Els2* gene [49]. (**B**) The high-resolution genetic map of the *Els2* gene. (**C**) The corresponding physical location of the polymorphic linkage markers of the *Els2* gene.

2.2. Development of KASP Markers Based on the 660K SNP Array

To saturate marker density in the *Els2* region, we combined bulked segregant analysis (BSA) with 660K SNP arrays. A total of 10,097 SNP loci from the 660K SNP array were polymorphic between the two bulks and were located on 21 chromosomes, of which 3449 were located on chromosome 2B and the others were distributed on the other chromosomes (Figure 3A). These results were consistent with the previous 90K SNP genotyping result [49]. Of the 3449 SNP loci located on 2B, more than 1100 were positioned in the interval 750–775 Mb according to the wheat genome assembly (Figure 3B). Furthermore, two *Els2*-flanking KASP markers were located in the region 750–775 Mb (Figure 2A,C). To develop molecular markers more tightly linked to the *Els2* gene, 25 SNPs located within the interval between BS00084417_51 and RFL_Contig4423_529 (763–772 Mb) were selected for conversion to KASP markers. The results indicated that nine KASP markers were tightly linked to the *Els2* gene (Figure 1B,D, Table 1).

2.3. Construction of a High-Resolution Genetic Linkage Map

To construct a high-resolution genetic linkage map of *Els2*, we developed a large F2 population of 838 plants. The F_2 population showed three classes of trait distribution, of which 198 were wide type plants, 419 were intermediate plants and 213 were mutant plants. The χ^2 test shows a separation ratio of 1:2:1 ($\chi^2 = 0.53 < \chi^2_{0.05,2} = 5.99$), which were consistent with our previous observations [49].

The *Els2*-flanking KASP markers BS00084417_51 and RFL_Contig4423_529 were used to identify recombinants in the F_2 mapping population of the LF2099 × Chinese Spring cross. Only nine recombinant individuals were identified from 838 F_2 individuals. Other molecular markers, including the previously reported IP markers 2BIP06, 2BIP12 and 2BIP17 [49], were then analyzed with these

recombinants only. The $F_{2:3}$ families produced by selfing the recombinant F_2 plants were used to further estimate phenotypes. In combination with the marker genotypes and recombinant phenotype, a high-resolution genetic map around the *Els2* locus was eventually constructed (Figure 2B). Among the markers flanking the *Els2* gene, the KASP markers AX-111643885 and AX-111128667 were the most closely linked, at distances of 0.12 and 0.12 cM, respectively. Two KASP markers, AX-109407129 and AX-95682571, co-segregated with the *Els2* gene.
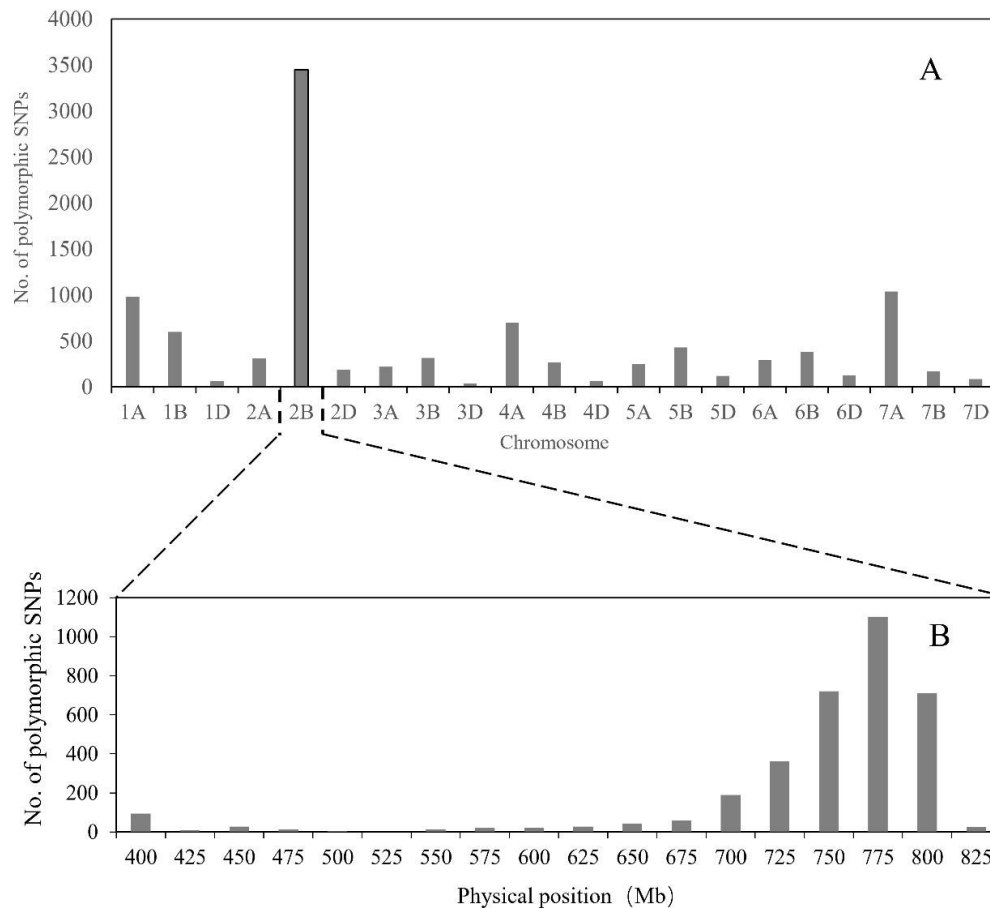

Figure 3. Number of polymorphic single nucleotide polymorphisms (SNP) distributed on different wheat chromosomes (**A**) and distribution of SNP variants on chromosome 2B (**B**).

2.4. Physical Mapping and Gene Annotation of the Els2 Goal Interval

To determine the physical locations of the *Els2*-linked markers, the sequences of all markers anchored in the high-resolution genetic map were used to blast against the Chinese Spring genomic sequence, and the relative physical positions of those markers were generally consistent with the genetic linkage map (Figure 2B,C). The genetic region of the markers AX-111643885 and AX-111128667 corresponded to a 1.61 Mb (764913189–766527697) genomic interval in the Chinese Spring reference genome (Figure 2C) and contained 27 annotated protein-coding genes (Table 2). Among them, one 50S ribosomal protein L14, five cytochrome P450 family proteins, three cysteine proteinases, two serine/threonine-protein kinase, and one RECEPTOR-like protein kinase were identified.

Table 2. Gene models between the two flanking markers AX-111643885 and AX-111128667 based on the International Wheat Genome Consortium (IWGSC) RefSeq v1.1 annotation.

Gene	Annotation
TraesCS2B02G575700.1	DEAD-box ATP-dependent RNA helicase 52A
TraesCS2B02G575800.1	CC-NBS-LRR family disease resistance protein
TraesCS2B02G575900.1	50S ribosomal protein L14
TraesCS2B02G576000.2	OTU domain-containing protein, putative
TraesCS2B02G576100.2	Calreticulin-like protein
TraesCS2B02G576200.1	cysteine-rich RLK (RECEPTOR-like protein kinase) 29
TraesCS2B02G576300.1	Cysteine proteinase
TraesCS2B02G576400.1	Serine/threonine-protein kinase
TraesCS2B02G576500.1	Myb family transcription factor family protein
TraesCS2B02G576600.2	lectin-receptor kinase
TraesCS2B02G576700.1	Cytochrome P450
TraesCS2B02G576800.1	RING/U-box superfamily protein
TraesCS2B02G576900.1	Chromosome segregation in meiosis protein 3
TraesCS2B02G577000.1	RING/U-box superfamily protein
TraesCS2B02G577100.1	Cytochrome P450 family protein, expressed
TraesCS2B02G577200.1	Cytochrome P450 family protein, expressed
TraesCS2B02G577300.1	Cysteine proteinase
TraesCS2B02G577400.1	Cytochrome P450 family protein, expressed
TraesCS2B02G577500.1	Cysteine proteinase
TraesCS2B02G577600.1	Serine/threonine-protein phosphatase 7 long form-like protein
TraesCS2B02G577700.1	Phytol kinase 1
TraesCS2B02G577800.1	Exostosin family protein
TraesCS2B02G577900.1	B3 domain-containing protein
TraesCS2B02G578000.1	Polyadenylate-binding protein 1-B-binding protein
TraesCS2B02G578100.1	ATP-dependent Clp protease proteolytic subunit 3
TraesCS2B02G578200.4	Serine/threonine-protein kinase
TraesCS2B02G578300.1	Cytochrome P450, putative

3. Discussion

Mapping functional genes using ethyl methanesulfonate (EMS) mutants combined with map-based cloning has been applied in many crops; however, the high-resolution mapping of a mutant gene in wheat may become problematic and tedious without high-density molecular markers. Several approaches have been used to develop high-density molecular markers around the target gene. Comparative genomics analyses are traditional and effective approaches for marker development in a wheat positional cloning project [50]. By applying comparative genomics analyses, we previously developed five new markers linked to the *Els2* gene [49]. Although release of the Chinese Spring whole genomic assembly sequences [51] would reduce the importance of comparative genomics analyses in marker development, it is still an effective method for other species without a reference genome sequence.

The SNP genotyping assays, namely 90K [38] and 660K [42], have opened a new way to undertake a more efficient and faster marker saturation of target genes in wheat [47]. Compared to the 90K SNP chip, the 660K chip has several advantages, such as higher marker density and higher resolution, as well as a better distribution on the chromosomes [42,44]. In the present study, we used the 660K chip to screen candidate markers linked to *Els2* and a significant number of polymorphic SNPs were identified (Figure 3A,B). To improve the efficiency of genotyping individuals, polymorphic SNP markers on 2BL were converted to KASP markers to genotype the F_2 population. Using this strategy, the *Els2* locus was further narrowed down to a 1.61 Mb region in the Chinese Spring chromosome 2BL containing 27 predicted genes with high confidence (Figure 2B,C, Table 2). It was a clearly effective approach to exploit constantly the updated genome information and high-throughput SNP platforms for high-resolution mapping of a mutant gene in wheat. In addition to the methods used in our study, the combination of the BSA strategy with next-generation sequencing technology (RNA-Seq or exome

sequencing) has been used as a mapping strategy that offers the promise of a rapid discovery of genetic markers linked to target genes in wheat [3,52,53].

The *Els2* genomic interval was narrowed down to the 1.61 Mb interval of the Chinese Spring 2BL containing 27 predicted protein-coding genes. Some of the annotated genes were associated with plant early leaf senescence, including the 50S ribosomal protein L14, cytochrome P450 family proteins, cysteine proteinase, serine/threonine-protein kinase, and RECEPTOR-like protein kinase (Table 2). In rice, the gene encoding the 50S ribosomal protein L21 in the chloroplastic precursor 50S ribosomal protein may be responsible for the early senescence mutant *es-t* [54]. Cytochrome P450 CYP89A9, which is in charge of non-fluorescent dioxobilin-type chlorophyll catabolite accumulation, is drawn into the formation of major chlorophyll catabolites during leaf senescence [55]. Cysteine proteases are the most abundant enzymes responsible for the proteolytic activity during leaf senescence [56]. A number of cDNA clones encoding cysteine proteinases in different plants have been previously reported to be up-regulated during leaf senescence [57]. Protein kinases and autophagy-related genes were also reported to play an important role in leaf senescence [58].

In the present study, we reported our work on the high-resolution genetic mapping of the novel early leaf senescence gene *Els2*. First, the development of 12 KASP markers from the high-density SNP arrays enabled us to construct high-resolution genetic maps around the target locus. Second, we physically delimited the *Els2* gene to a 1.61-Mb genomic region including 27 putative genes. We believe our study has made a solid foundation for the future isolation of the *Els2* locus.

4. Materials and Methods

4.1. Plant Materials and Population Construction

The novel early leaf senescence mutant LF2099 was identified from the chemical mutagen EMS-induced library derived from the common wheat accession H261. To develop a saturated genetic linkage map for *Els2*, the F_2 and $F_{2:3}$ mapping populations (consisting of 838 lines) produced by crossing LF2099 to the normal leaf senescence cultivar Chinese Spring were used throughout the study. All plants were grown on the experimental farm of Northwest A&F University, Yangling, China. Leaf senescence phenotypes were evaluated by visual observation. To ensure the accuracy of the results, the phenotypes of the recombinant F_2 individuals were further validated by using the F_3 lines. The F_3 lines containing 30 seeds from every F_2 plant were planted in rows to verify the phenotypes of the F_2 plants in fields.

4.2. Combined Bulked Segregant Analysis Using the 660K SNP Array

The total genomic DNA from the parents and F_2 plants were isolated from leaves by using a cetyltrimethylammonium bromide (CTAB) method [59]. The DNA quantity was measured spectrophotometrically, and the DNA integrity was confirmed on agarose gel. To obtain closer SNP markers and saturate the targeted gene, BSA was performed to identify polymorphic markers between the early and normal DNA bulks. The DNA of the 12 homozygous plants that exhibited early leaf senescence and normal leaf senescence, based on a validation of the phenotypes of the F_3 family, was pooled to construct an early bulk sample and a normal bulk sample, separately. The F_2 bulks were genotyped with the 660K SNP arrays from CapitalBio Corporation (Beijing, China) using the Affymetrix GeneTitan System based on the Axiom 2.0 Assay Manual Workflow protocol. Allele calling was performed using the Affymetrix proprietary software according to Axiom Best Practices Genotyping Workflow. The sequences of all SNPs were used to blast version1.0 of the assembled Chinese Spring survey sequence (International Wheat Genome Consortium (IWGSC) RefSeq v1.0) to determine their physical positions [51].

4.3. Conversion of SNP Markers to KASP Markers

The polymorphic SNP markers from 90K and 660K were converted to KASP markers using the PolyMarker software (available online: http://polymarker.tgac.ac.uk) [60]. Chromosome-specific KASP markers were used to screen the parents and small population to confirm the polymorphisms before genotyping the entire mapping population. The KASP reactions were performed in a 384-well plate format following the protocol of LGC Genomics. Each KASP reaction mixtures consisted of final volumes of 5 μL containing 50–100 ng of genomic DNA, 2.5 μL of 2 × KASP Master mix (V4.0, LGC Genomics, Hoddesdon, UK), 0.056 μL of assay primer mix (12 μM of each allele-specific primer and 30 μM of common primer) and 2.444 μL of water. The assay reaction was performed in a 384 well Thermal Cycler (Bio-Rad) in the following cycling conditions: denaturation at 95 °C for 15 min, 9 cycles of 95 °C for 20 s and touchdown starting at 65 °C for 60 s (decreased by 0.8 °C per cycle), 30–40 cycles of amplification (95 °C for 20 s; 57 °C for 60 s). The amplified products were visualized by a microplate reader (FLUOstar Omega, BMG LABTECH, Germany) and analyzed by the software Klustering Caller (LGC, Middlesex, UK) [61].

4.4. Construction of High-Density Genetic Linkage Map

The linkage analysis of the polymorphic molecular markers and the *Els2* gene was conducted using JoinMap4.0 software [62] with default parameters and a LOD score of 3.0 as a threshold. The genetic distance was calculated and presented in Kosambi centiMorgans (cM). The genetic map was drawn with the software Mapdraw V2.1 (Huazhong Agricultural Sciences, Wuhan, China) [63].

4.5. Physical Mapping and Gene Annotation of the Els2 Region

All 14 markers used for the fine mapping of the *Els2* were anchored to the wheat reference genome sequence [51]. All sequences including forward and reverse primers were searched against the Chinese Spring whole genome assembly sequences (Reference Sequence v1.0, IWGSC, http://www.wheatgenome.org/) using the BLASTN algorithm applying default parameters. Obtained physical positions of mapped markers were visualized using the software Mapdraw V2.1 (Huazhong Agricultural Sciences, Wuhan, China) [63]. The information on the Chinese Spring genomic sequence was used to identify the genes that were included in the interval between the two *Els2*-flanking markers. IWGSC RefSeq v1.1 with gene annotations became available on the website https://wheat-urgi.versailles.inra.fr/Seq-Repository/Annotation. Annotated genes in the target region were extracted for analyzing genes involved in plant leaf senescence.

Author Contributions: Conceptualization, Y.X. and C.W.; methodology, N.W., Y.X., S.L. and Y.G.; software, N.W.; validation, N.W. and Y.X.; formal analysis, N.W. and Y.X.; investigation, Y.L. and S.W.; resources, C.W.; data curation, S.W., Y.L., and S.L.; writing—original draft, Y.X., N.W., S.L. and S.W.; writing—review and editing, Y.L. and Y.G.; supervision, and funding acquisition, C.W. All authors have read and agreed to the published version of the manuscript.

Conflicts of Interest: The authors declare no conflict of interest.

References

1.　Fu, D.L.; Uauy, C.; Distelfeld, A.; Blechl, A.; Epstein, L.; Chen, X.M.; Sela, H.A.; Fahima, T.; Dubcovsky, J. A Kinase-START Gene Confers Temperature-Dependent Resistance to Wheat Stripe Rust. *Science* **2009**, *323*, 1357–1360. [CrossRef]

2.　Sylvester-Bradley, R.; Scott, R.; Wright, C. Physiology in the production and improvement of cereals. In *Physiology in the Production and Improvement of Cereals*; HGCA: London, UK, 1990.

3.　Li, M.M.; Li, B.B.; Guo, G.H.; Chen, Y.X.; Xie, J.Z.; Lu, P.; Wu, Q.H.; Zhang, D.Y.; Zhang, H.Z.; Yang, J.; et al. Mapping a leaf senescence gene *els1* by BSR-Seq in common wheat. *Crop J.* **2018**, *6*, 236–243. [CrossRef]

4. Woo, H.R.; Kim, H.J.; Lim, P.O.; Nam, H.G. Leaf Senescence: Systems and Dynamics Aspects. *Annu. Rev. Plant Biol.* **2019**, *70*, 347–376. [CrossRef] [PubMed]

5. Kim, J.; Woo, H.R.; Nam, H.G. Toward Systems Understanding of Leaf Senescence: An Integrated Multi-Omics Perspective on Leaf Senescence Research. *Mol. Plant* **2016**, *9*, 813–825. [CrossRef] [PubMed]

6. Pattanayak, G.K.; Tripathy, B.C. Modulation of biosynthesis of photosynthetic pigments and light-harvesting complex in wild-type and gun5 mutant of *Arabidopsis thaliana* during impaired chloroplast development. *Protoplasma* **2016**, *253*, 747–752. [CrossRef]

7. Morita, R.; Sato, Y.; Masuda, Y.; Nishimura, M.; Kusaba, M. Defect in non-yellow coloring 3, an alpha/beta hydrolase-fold family protein, causes a stay-green phenotype during leaf senescence in rice. *Plant J.* **2009**, *59*, 940–952. [CrossRef]

8. Rong, H.; Tang, Y.; Zhang, H.; Wu, P.; Chen, Y.; Li, M.; Wu, G.; Jiang, H. The Stay-Green Rice like (*SGRL*) gene regulates chlorophyll degradation in rice. *J. Plant Physiol.* **2013**, *170*, 1367–1373. [CrossRef]

9. Yamatani, H.; Sato, Y.; Masuda, Y.; Kato, Y.; Morita, R.; Fukunaga, K.; Nagamura, Y.; Nishimura, M.; Sakamoto, W.; Tanaka, A.; et al. *NYC4*, the rice ortholog of *Arabidopsis THF1*, is involved in the degradation of chlorophyll-protein complexes during leaf senescence. *Plant J.* **2013**, *74*, 652–662. [CrossRef]

10. Wang, M.; Zhang, T.; Peng, H.; Luo, S.; Tan, J.; Jiang, K.; Heng, Y.; Zhang, X.; Guo, X.; Zheng, J.; et al. Rice premature leaf senescence 2, encoding a glycosyltransferase (GT), is involved in leaf senescence. *Front. Plant Sci.* **2018**, *9*, 560. [CrossRef]

11. Wang, Z.; Wang, Y.; Hong, X.; Hu, D.; Liu, C.; Yang, J.; Li, Y.; Huang, Y.; Feng, Y.; Gong, H.; et al. Functional inactivation of UDP-N-acetylglucosamine pyrophosphorylase 1 (*UAP1*) induces early leaf senescence and defence responses in rice. *J. Exp. Bot.* **2015**, *66*, 973–987. [CrossRef]

12. Chen, L.J.; Wuriyanghan, H.; Zhang, Y.Q.; Duan, K.X.; Chen, H.W.; Li, Q.T.; Lu, X.; He, S.J.; Ma, B.; Zhang, W.K.; et al. An S-domain receptor-like kinase, *OsSIK2*, confers abiotic stress tolerance and delays dark-induced leaf senescence in rice. *Plant Physiol.* **2013**, *163*, 1752–1765. [CrossRef] [PubMed]

13. Bi, Z.; Zhang, Y.; Wu, W.; Zhan, X.; Yu, N.; Xu, T.; Liu, Q.; Li, Z.; Shen, X.; Chen, D.; et al. *ES7*, encoding a ferredoxin-dependent glutamate synthase, functions in nitrogen metabolism and impacts leaf senescence in rice. *Plant Sci.* **2017**, *259*, 24–34. [CrossRef] [PubMed]

14. Takei, K.; Ueda, N.; Aoki, K.; Kuromori, T.; Hirayama, T.; Shinozaki, K.; Yamaya, T.; Sakakibara, H. *AtIPT3* is a key determinant of nitrate-dependent cytokinin biosynthesis in *Arabidopsis*. *Plant Cell Physiol.* **2004**, *45*, 1053–1062. [CrossRef] [PubMed]

15. Kang, J.; Turano, F.J. The putative glutamate receptor 1.1 (*AtGLR1.1*) functions as a regulator of carbon and nitrogen metabolism in *Arabidopsis thaliana*. *Proc. Natl. Acad. Sci. USA* **2003**, *100*, 6872–6877. [CrossRef]

16. Zhao, Y.; Chan, Z.; Gao, J.; Xing, L.; Cao, M.; Yu, C.; Hu, Y.; You, J.; Shi, H.; Zhu, Y.; et al. ABA receptor *PYL9* promotes drought resistance and leaf senescence. *Proc. Natl. Acad. Sci. USA* **2016**, *113*, 1949–1954. [CrossRef] [PubMed]

17. Takasaki, H.; Maruyama, K.; Takahashi, F.; Fujita, M.; Yoshida, T.; Nakashima, K.; Myouga, F.; Toyooka, K.; Yamaguchi-Shinozaki, K.; Shinozaki, K. SNAC-As, stress-responsive *NAC* transcription factors, mediate ABA-inducible leaf senescence. *Plant J.* **2015**, *84*, 1114–1123. [CrossRef]

18. Liang, C.; Wang, Y.; Zhu, Y.; Tang, J.; Hu, B.; Liu, L.; Ou, S.; Wu, H.; Sun, X.; Chu, J.; et al. *OsNAP* connects abscisic acid and leaf senescence by fine-tuning abscisic acid biosynthesis and directly targeting senescence-associated genes in rice. *Proc. Natl. Acad. Sci. USA* **2014**, *111*, 10013–10018. [CrossRef]

19. Yu, J.; Zhang, Y.X.; Di, C.; Zhang, Q.L.; Zhang, K.; Wang, C.C.; You, Q.; Yan, H.; Dai, S.Y.; Yuan, J.S.; et al. *JAZ7* negatively regulates dark-induced leaf senescence in *Arabidopsis*. *J. Exp. Bot.* **2016**, *67*, 751–762. [CrossRef]

20. Lee, I.C.; Hong, S.W.; Whang, S.S.; Lim, P.O.; Nam, H.G.; Koo, J.C. Age-Dependent Action of an ABA-Inducible Receptor Kinase, *RPK1*, as a Positive Regulator of Senescence in *Arabidopsis* Leaves. *Plant Cell Physiol.* **2011**, *52*, 651–662. [CrossRef]

21. Zhang, Q.; Xia, C.; Zhang, L.; Dong, C.; Liu, X.; Kong, X. Transcriptome Analysis of a Premature Leaf Senescence Mutant of Common Wheat (*Triticum aestivum* L.). *Int. J. Mol. Sci.* **2018**, *19*, 782. [CrossRef]

22. Borrill, P.; Harrington, S.A.; Simmonds, J.; Uauy, C. Identification of Transcription Factors Regulating Senescence in Wheat through Gene Regulatory Network Modelling. *Plant Physiol.* **2019**, *180*, 1740–1755. [CrossRef] [PubMed]

23. Gregersen, P.L.; Holm, P.B. Transcriptome analysis of senescence in the flag leaf of wheat (*Triticum aestivum* L.). *Plant Biotechnol. J.* **2007**, *5*, 192–206. [CrossRef] [PubMed]

24. Gregersen, P.L.; Holm, P.B.; Krupinska, K. Leaf senescence and nutrient remobilisation in barley and wheat. *Plant Biol.* **2008**, *10*, 37–49. [CrossRef] [PubMed]

25. Agarwal, P.; Jaiswal, V.; Kumar, S.; Balyan, H.S.; Gupta, P.K. Chromosome mapping of four novel mutants in bread wheat (*Triticum aestivum* L.). *Acta Physiol. Plant* **2015**, *37*, 66. [CrossRef]

26. Harrington, S.A.; Cobo, N.; Karafiatova, M.; Dolezel, J.; Borrill, P.; Uauy, C. Identification of a Dominant Chlorosis Phenotype Through a Forward Screen of the *Triticum turgidum* cv. Kronos TILLING Population. *Front. Plant Sci.* **2019**, *10*, 963. [CrossRef]

27. Ansari, M.J.; Al-Ghamdi, A.; Usmani, S.; Kumar, R.; Nuru, A.; Singh, K.; Dhaliwal, H.S. Characterization and gene mapping of a brittle culm mutant of diploid wheat (*Triticum monococcum* L.) with irregular xylem vessels development. *Acta Physiol. Plant* **2013**, *35*, 2407–2419. [CrossRef]

28. Li, N.; Jia, J.; Xia, C.; Liu, X.; Kong, X. Characterization and mapping of novel chlorophyll deficient mutant genes in durum wheat. *Breed Sci.* **2013**, *63*, 169–175. [CrossRef]

29. Xu, T.; Bian, N.; Wen, M.; Xiao, J.; Yuan, C.; Cao, A.; Zhang, S.; Wang, X.; Wang, H. Characterization of a common wheat (*Triticum aestivum* L.) high-tillering dwarf mutant. *Theor. Appl. Genet.* **2017**, *130*, 483–494. [CrossRef]

30. Ansari, M.J.; Al-Ghamdi, A.; Kumar, R.; Usmani, S.; Al-Attal, Y.; Nuru, A.; Mohamed, A.A.; Singh, K.; Dhaliwal, H.S. Characterization and gene mapping of a chlorophyll-deficient mutant *clm1* of *Triticum monococcum* L. *Biol. Plant.* **2013**, *57*, 442–448. [CrossRef]

31. Zhang, L.L.; Liu, C.; An, X.Y.; Wu, H.Y.; Feng, Y.; Wang, H.; Sun, D.J. Identification and genetic mapping of a novel incompletely dominant yellow leaf color gene, Y1718, on chromosome 2BS in wheat. *Euphytica* **2017**, *213*, 141. [CrossRef]

32. Brenchley, R.; Spannagl, M.; Pfeifer, M.; Barker, G.L.; D'Amore, R.; Allen, A.M.; McKenzie, N.; Kramer, M.; Kerhornou, A.; Bolser, D.; et al. Analysis of the bread wheat genome using whole-genome shotgun sequencing. *Nature* **2012**, *491*, 705–710. [CrossRef] [PubMed]

33. Luo, M.C.; Gu, Y.Q.; Puiu, D.; Wang, H.; Twardziok, S.O.; Deal, K.R.; Huo, N.; Zhu, T.; Wang, L.; Wang, Y.; et al. Genome sequence of the progenitor of the wheat D genome *Aegilops tauschii*. *Nature* **2017**, *551*, 498–502. [CrossRef] [PubMed]

34. Cui, F.; Zhang, N.; Fan, X.L.; Zhang, W.; Zhao, C.H.; Yang, L.J.; Pan, R.Q.; Chen, M.; Han, J.; Zhao, X.Q.; et al. Utilization of a Wheat660K SNP array-derived high-density genetic map for high-resolution mapping of a major QTL for kernel number. *Sci. Rep.* **2017**, *7*, 3788. [CrossRef] [PubMed]

35. Jia, J.; Zhao, S.; Kong, X.; Li, Y.; Zhao, G.; He, W.; Appels, R.; Pfeifer, M.; Tao, Y.; Zhang, X.; et al. *Aegilops tauschii* draft genome sequence reveals a gene repertoire for wheat adaptation. *Nature* **2013**, *496*, 91–95. [CrossRef] [PubMed]

36. Lai, K.; Duran, C.; Berkman, P.J.; Lorenc, M.T.; Stiller, J.; Manoli, S.; Hayden, M.J.; Forrest, K.L.; Fleury, D.; Baumann, U.; et al. Single nucleotide polymorphism discovery from wheat next-generation sequence data. *Plant Biotechnol. J.* **2012**, *10*, 743–749. [CrossRef] [PubMed]

37. Cavanagh, C.R.; Chao, S.; Wang, S.; Huang, B.E.; Stephen, S.; Kiani, S.; Forrest, K.; Saintenac, C.; Brown-Guedira, G.L.; Akhunova, A.; et al. Genome-wide comparative diversity uncovers multiple targets of selection for improvement in hexaploid wheat landraces and cultivars. *Proc. Natl. Acad. Sci. USA* **2013**, *110*, 8057–8062. [CrossRef]

38. Wang, S.; Wong, D.; Forrest, K.; Allen, A.; Chao, S.; Huang, B.E.; Maccaferri, M.; Salvi, S.; Milner, S.G.; Cattivelli, L.; et al. Characterization of polyploid wheat genomic diversity using a high-density 90,000 single nucleotide polymorphism array. *Plant Biotechnol. J.* **2014**, *12*, 787–796. [CrossRef]

39. Winfield, M.O.; Allen, A.M.; Burridge, A.J.; Barker, G.L.; Benbow, H.R.; Wilkinson, P.A.; Coghill, J.; Waterfall, C.; Davassi, A.; Scopes, G.; et al. High-density SNP genotyping array for hexaploid wheat and its secondary and tertiary gene pool. *Plant Biotechnol. J.* **2016**, *14*, 1195–1206. [CrossRef]

40. Klindworth, D.L.; Saini, J.; Long, Y.; Rouse, M.N.; Faris, J.D.; Jin, Y.; Xu, S.S. Physical mapping of DNA markers linked to stem rust resistance gene *Sr47* in durum wheat. *Theor. Appl. Genet.* **2017**, *130*, 1135–1154. [CrossRef]

41. Ren, T.; Hu, Y.; Tang, Y.; Li, C.; Yan, B.; Ren, Z.; Tan, F.; Tang, Z.; Fu, S.; Li, Z. Utilization of a Wheat55K SNP Array for Mapping of Major QTL for Temporal Expression of the Tiller Number. *Front. Plant Sci.* **2018**, *9*, 333. [CrossRef]

42. Sun, C.; Dong, Z.; Zhao, L.; Ren, Y.; Zhang, N.; Chen, F. The Wheat 660K SNP array demonstrates great potential for marker-assisted selection in polyploid wheat. *Plant Biotechnol. J.* **2020**. [CrossRef] [PubMed]

43. Sun, L.; Yang, W.; Li, Y.; Shan, Q.; Ye, X.; Wang, D.; Yu, K.; Lu, W.; Xin, P.; Pei, Z.; et al. A wheat dominant dwarfing line with *Rht12*, which reduces stem cell length and affects gibberellic acid synthesis, is a 5AL terminal deletion line. *Plant J.* **2019**, *97*, 887–900. [CrossRef] [PubMed]

44. Tian, X.; Wen, W.; Xie, L.; Fu, L.; Xu, D.; Fu, C.; Wang, D.; Chen, X.; Xia, X.; Chen, Q.; et al. Molecular Mapping of Reduced Plant Height Gene *Rht24* in Bread Wheat. *Front. Plant Sci.* **2017**, *8*, 1379. [CrossRef] [PubMed]

45. Wu, J.; Zeng, Q.; Wang, Q.; Liu, S.; Yu, S.; Mu, J.; Huang, S.; Sela, H.; Distelfeld, A.; Huang, L.; et al. SNP-based pool genotyping and haplotype analysis accelerate fine-mapping of the wheat genomic region containing stripe rust resistance gene *Yr26*. *Theor. Appl. Genet.* **2018**, *131*, 1481–1496. [CrossRef]

46. Wu, J.; Wang, Q.; Xu, L.; Chen, X.; Li, B.; Mu, J.; Zeng, Q.; Huang, L.; Han, D.; Kang, Z. Combining Single Nucleotide Polymorphism Genotyping Array with Bulked Segregant Analysis to Map a Gene Controlling Adult Plant Resistance to Stripe Rust in Wheat Line 03031-1-5 H62. *Phytopathology* **2017**, *108*, 103–113. [CrossRef]

47. Wu, J.; Wang, Q.; Liu, S.; Huang, S.; Mu, J.; Zeng, Q.; Huang, L.; Han, D.; Kang, Z. Saturation Mapping of a Major Effect QTL for Stripe Rust Resistance on Wheat Chromosome 2B in Cultivar Napo 63 Using SNP Genotyping Arrays. *Front. Plant Sci.* **2017**, *8*, 653. [CrossRef]

48. Jiang, H.B.; Wang, N.; Jian, J.T.; Wang, C.S.; Xie, Y.Z. Rapid mapping of a chlorina mutant gene cn-A1 in hexaploid wheat by bulked segregant analysis and single nucleotide polymorphism genotyping arrays. *Crop Pasture Sci.* **2019**, *70*, 827–836. [CrossRef]

49. Wang, N.; Xie, Y.Z.; Li, Y.Z.; Wu, S.N.; Wei, H.H.; Wang, C.S. Molecular mapping a novel early leaf-senescence gene *Els2* in common wheat by SNP genotyping arrays. *Crop Pasture Sci.* **2020**, *71*, 356–367. [CrossRef]

50. Wang, M.; Wang, S.; Xia, G. From genome to gene: A new epoch for wheat research? *Trends Plant Sci.* **2015**, *20*, 380–387. [CrossRef]

51. International Wheat Genome Sequencing Consortium (IWGSC). Shifting the limits in wheat research and breeding using a fully annotated reference genome. *Science* **2018**, *361*, eaar7191. [CrossRef]

52. Martinez, S.A.; Shorinola, O.; Conselman, S.; See, D.; Skinner, D.Z.; Uauy, C.; Steber, C.M. Exome sequencing of bulked segregants identified a novel *TaMKK3-A* allele linked to the wheat ERA8 ABA-hypersensitive germination phenotype. *Theor. Appl. Genet.* **2020**, *133*, 719–736. [CrossRef] [PubMed]

53. Hu, J.H.; Li, J.T.; Wu, P.P.; Li, Y.H.; Qiu, D.; Qu, Y.F.; Xie, J.Z.; Zhang, H.J.; Yang, L.; Fu, T.T.; et al. Development of SNP, KASP, and SSR Markers by BSR-Seq Technology for Saturation of Genetic Linkage Map and Efficient Detection of Wheat Powdery Mildew Resistance Gene *Pm61*. *Int. J. Mol. Sci.* **2019**, *20*, 750. [CrossRef] [PubMed]

54. Yang, Y.; Rao, Y.; Liu, H.; Fang, Y.; Dong, G.; Huang, L.; Leng, Y.; Guo, L.; Zhang, G.; Hu, J.; et al. Characterization and fine mapping of an early senescence mutant (*es-t*) in *Oryza sativa* L. *Chin. Sci. Bull.* **2011**, *56*, 2437–2443. [CrossRef]

55. Christ, B.; Sussenbacher, I.; Moser, S.; Bichsel, N.; Egert, A.; Muller, T.; Krautler, B.; Hortensteiner, S. Cytochrome P450 CYP89A9 Is Involved in the Formation of Major Chlorophyll Catabolites during Leaf Senescence in *Arabidopsis*. *Plant Cell* **2013**, *25*, 1868–1880. [CrossRef]

56. Diaz-Mendoza, M.; Velasco-Arroyo, B.; Gonzalez-Melendi, P.; Martinez, M.; Diaz, I. C1A cysteine protease-cystatin interactions in leaf senescence. *J. Exp. Bot.* **2014**, *65*, 3825–3833. [CrossRef]

57. Chen, G.H.; Huang, L.T.; Yap, M.N.; Lee, R.H.; Huang, Y.J.; Cheng, M.C.; Chen, S.C. Molecular characterization of a senescence-associated gene encoding cysteine proteinase and its gene expression during leaf senescence in sweet potato. *Plant Cell Physiol.* **2002**, *43*, 984–991. [CrossRef]

58. Zhou, C.; Cai, Z.; Guo, Y.; Gan, S. An *arabidopsis* mitogen-activated protein kinase cascade, *MKK9-MPK6*, plays a role in leaf senescence. *Plant Physiol.* **2009**, *150*, 167–177. [CrossRef]

59. Doyle, J.J.T.; Doyle, J.L. Isolation of Plant DNA from fresh tissue. *Focus* **1990**, *12*, 13–15.

60. Ramirez-Gonzalez, R.H.; Uauy, C.; Caccamo, M. PolyMarker: A fast polyploid primer design pipeline. *Bioinformatics* **2015**, *31*, 2038–2039. [CrossRef]

61. Wu, J.; Liu, S.; Wang, Q.; Zeng, Q.; Mu, J.; Huang, S.; Yu, S.; Han, D.; Kang, Z. Rapid identification of an adult plant stripe rust resistance gene in hexaploid wheat by high-throughput SNP array genotyping of pooled extremes. *Theor. Appl. Genet.* **2018**, *131*, 43–58. [CrossRef]

62.　Van Ooijen, J.W. JoinMap®4, Software for the Calculation of Genetic Linkage Maps in Experimental Populations. Available online: https://www.scienceopen.com/document?vid=baa76c8c-fb55-4c13-a6ca-24c71002ab5a (accessed on 15 December 2006).

63.　Liu, R.H.; Meng, J.L. MapDraw:A Microsoft Excel Macro for Drawing Genetic Linkage Maps Based on Given Genetic Linkage Data. *Hereditas* **2003**, *25*, 317–321. [PubMed]